Original Article
Retrograde-tracing and immunohistochemical study of sympathetic ganglia to the csa rabbit model

Hui Gou[1*], Yuan Jiang[1*], Sanrong Wang[1], Yang Sun[2], Lehua Yu[1]

[1]Department of Rehabilitation Medicine and Physical Therapy, China; [2]Institute of Ultrasound Imaging, The Second Affiliated Hospital, Chongqing Medical University, Chongqing, China. *Equal contributors.

Abstract: Injecting sclerosing agent next to parapophysis of cervical vertebra is a practical method to produce cervical spondylosis of vertebral artery type (CSA) rabbit model. The purpose of this study was to explore the functions of sympathetic trunk nerve in this kind of CSA rabbit models. The rabbits were randomly divided into CSA group and control group. Transcranial Doppler (TCD) was used to detect the peak systolic velocity (PSV), end diastolic velocity (EDV), mean velocity (Vm), pulsatile index (Pi), resistance index (RI) of the vertebral artery after the sclerosing agent was injected next to the right side parapophysis of cervical vertebra in the CSA group. To further investigate the effect of different lesion in neck soft tissues and cervical facet on the functions of sympathetic trunk nerve, fluorescent tracer fast blue (FB) was injected in hypoderm, upper trapezius muscle and next to parapophysis of C3-C5 sections, and combined fluorescent histochemical staining to observe the FB-positive neurons co-expressed neuropeptide Y (NPY) and tyrosine hydroxylase (TH)-immunoreactivity in right side sympathetic trunk ganglia (STG), and western blotting assay was used to detect the protein expressions of NPY and TH. The results showed that light blue fluorescence surrounding the interior walls and adventitia of the right side vertebral artery in CSA rabbits. The percentage of FB-positive neurons co-expressed NPY and TH-immunoreactivity and protein expression of NPY and TH in CSA rabbits was significant higher than those in the normal rabbits. Cervical facet lesion is a possible mechanism of the severe vertebral artery spasm and stenosis induced by the sympathetic nerve around vertebral artery was directly activated in CSA rabbits.

Keywords: Cervical spondylosis, retrograde-tracing, immunohistochemistry

Introduction

Cervical spondylosis is a common degenerative disease in clinic characterized by neck pain, numbness, parethesia [1] and cervical vertigo [2]. The important risk factors of cervical spondylosis are age, gender and occupation, especially the modern unhealthy lifestyle and increased work pressure, and the morbidity rate is increasing, while the onset age is decreasing. Cervical spondylosis of vertebral artery type (CSA) is one of the most common type of cervical spondylosis. Vertebral artery spasm and stenosis, leading to vertebribasilar insufficiency as the main clinical manifestation of CSA, are induced by some pathogenic factors that stimulate the extracranial vertebral arteries such as Luschka joint hyperplasia, cer-

vical facet jionts displacement and neck spasms. The etiology, pathogenesis and treatment of CSA have attracted wide attentions from scholars in and abroad. Some animals are used to build animal model for different types of cervical spondylosis [3-7]. Many methods for setting up animal model of CSA were reported. However, the animal studies on simulating CSA were limited due to the complex operation steps, long cycle time, diverse pathogenesis of CSA and low achievement ratio. Shou et al. [8] reported a new method for inducing CSA rabbit model by injecting sclerosing agent next to parapophysis of cervical vertebra, and demonstrated this method induced the imbalance of both static and dynamic spinal forces as result of cervical degeneration. This method can effectively simulate the pathogenesis of CSA.

However, the functions of sympathetic trunk nerve in this kind of CSA rabbit model after injecting sclerosing agent is still unknown. The purpose of this study was to rebuild this kind of CSA rabbit models and further evaluate the functions of sympathetic trunk nerve.

Material and methods

Animals

All animal experimental protocol and care were approved by the Institutional Animal Care and Use Committee of Chongqing Medical University. Totally, 32 male New Zealand rabbits were employed, aged 6 months, weighing 2.5-3.0 kg and maintained under a controlled environmental conditions (12-hour light-dark cycle, temperature 22°C with humidity of 50%±5%). All rabbits were unrestricted access to water and food. After one week of acclimatization, rabbits were randomly divided into two groups: the control group (n=24) and the CSA group (n=8).

Establishment of CSA animal model

A total of 8 rabbits of CSA group were operated as Shou et al. [8] and with some reform. Briefly, after the rabbits were intramuscularly anesthetized with pentobarbital sodium (sigma-aldrich) at a dose of 50 mg/kg, the hair on the right pillow and neck of rabbits was removed with hair removal cream (VEET), and skin was sterilized. Then, 3 ml of sclerosing agent (Xiaozhiling injection, the component as follows: tannin, alum, sodium citrate, sodium bisulfate, trichloro-tert-butyl alcohol, glycerol, low molecular weight dextran injection, An Yi Pharmaceutical Ltd. Co.) was injected into the right side of third to fifth cervical vertebra (C3 to C5) next to the edge of transverse process with syringe needle, and the needle was left in injection place for about 60 s to avoid sclerosing agent leakage. Musculoskeletal ultrasound (MSUS) was used to guide accurate placement of the needle in injection protocol, and repeated at the 1st day of the next three weeks, respectively. The rabbits in the control group were not operated as above.

Transcranial doppler sonography (TCD)

The TCD detection was performed at 4 weeks of last injection of sclerosing agent. The probe head of TCD aligned to the right side of cervical vertebrae or pillow window, the direction angle and the focusing depth was 30-45° and 40-80 mm, respectively. Peak systolic velocity (PSV), end diastolic velocity (EDV), mean velocity (Vm), pulsatile index (Pi), resistance index (RI) of the vertebral artery were recorded. Totally, 8 normal rabbits were randomly selected in control group, and then those rabbits and 8 CSA rabbits were operated above TCD detection.

Fluorescent tracer fast blue injection method

After TCD detection, the rabbits in control group (n=24) were randomly divided into A group (n=8), B group (n=8), and C group (n=8). The CSA rabbits in CSA group were divided into D group (n=8). Then, all rabbits of four groups were injected fluorescent tracer Fast Blue (FB, Sigma-Aldrich, 2% aqueous solution). Briefly, the rabbits were intramuscularly anesthetized with pentobarbital sodium and skin of neck was sterilized. In A group, 50 μl of FB were carefully hypodermicaly injected into the right side hypoderm of C3 to C5 cervical vertebra; In B group, 50 μl of FB were carefully injected in the right side upper trapezius muscle of C3 to C5 cervical vertebra; In C group and D group, 50 μl of FB were carefully injected into parapophysis of C3 to C5 cervical vertebra (three sites) of right side with a manually operating glass Hamilton microsyringe. MSUS were used to guide accurate placement of the needle in above injection protocols, and the needle was left in the injection place for about 60 s to avoid FB leakage.

Tissue preparation

After FB injection for 24 h, the rabbits in each group were intramuscularly anesthetized with pentobarbital sodium. The rabbits were positioned in supine position and the surgical field was prepared with hair removal cream and Betadine scrub, and then a midline 10-12 cm longitudinal incision was performed. Thoracic diaphragm was broken to visualization of the heart. Normal saline (500 ml), 800-1000 ml phosophate buffer saline (PBS) containing paraformaldehyde (20 g/L) and glutaraldehyde (12.5 g/L) and 500 ml PBS containing sucrose (50 g/L) were poured into the heart in sequence. The right side vertebral artery of C3 to C5 cervical vertebrae were taken out and right side sympathetic trunk ganglia (STG) tissue samples were collected, include cervical, thoracic and

lumbar STG. All the tissue samples collected were fixed in 4% paraformaldehyde at 4°C for 6 h, rinsed in PBS and stored at 4°C in PBS containing 30% sucrose. The 5 of 8 right side STG tissue samples were selected from each group to put into the opti-mum cutting temperature compound (O.C.T compound, SAKURA) and quick freezing, then placed flat in the cryostat mould and cut into serial sections with cryostat. The thickness of each section was 20 µm. The sections were mounted on adhesion microscope slides (CITOGLAS, China) and without coverslip.

FB staining and quantitative analysis

The serial sections of each group were observed under a fluorescent microscope (Olympus ZX-004). The parameter of excitation wavelength was 390-420 nm and emission wavelength was 450 nm. If the neuronal cytoplasm was labeled blue fluorescence and the cell nucleus was recognizable in the section, it was named as FB-positive neuron. The number of FB-positive neurons were calculated by counting and analyzing with Abercrombie's formula [9, 10]. The correction factor of Abercrombie's formula is the 'T/T+h' ratio, and T= section thickness (20 µm), h= mean diameter of the nuclei of FB-positive neurons along the perpendicular axis to the plane of the section. A total of 100 FB-positive neurons were randomly selected for calculating the value of 'h'. Finally, the 'real' number of FB-positive neurons was equal to the arithmetic product of the raw count of FB-positive neurons and the correction factor.

Fluorescent histochemical staining

To investigate the occurrence of neuropeptide Y (NPY) and tyrosine hydroxylase (TH), a double labeling immunofluorescence method was used for observing serial sectionsof the STG. Briefly, the serial sections of four groups were dried and put into PBS containg 1% bovine serum albumin (BSA), 10% normal goat serum and 0.25% Triton X-100 (Solarbio, China) at room temperature (RT) for 1 h. Then, the serial sections were incubated with the primary antibody, polyclonal anti-neuropeptide Y (Abcam, ab6173) and monoclonal anti- tyrosine hydroxylase (Abcam, ab129991) at 4°C overnight. After incubated with a mixture solution containing flourescein isothiocyanate (FITC)-conjugated goat anti-rabbit IgG and biotinylated-goat anti-mouse IgG at RT for 1 h, the serial sections were further incubated with Texas Red-conjugated streptavidin at RT for 1 h. Finally, the labeled sections were observed and photographed with a fluorescent microscope. The fluorescence filters were interchanged by the observer for investigate the relationships between the FB-positive neurons and the neurons expressed NPY or TH-immunoreactivity in same visual field. The above observations were operated by the same observer.

Western blotting assay

To detect the protein expression of NPY and TH in the STG of each group, the rest of 3 right side STG tissue samples of each group were selected to extract total proteins. Briefly, the STG tissue samples were milled and lysed with RIPA lysis buffer (Beyotime, P0013B, China) for extracting total proteins. Protein samples were separated by sodium dodecyl sulfate-polyacrylamide gel electrophoresis, and then electrotransferred onto a polyvinylidene difluoride (PVDF) membrane. The PVDF membrane was blocked 2 h at RT in TBS-Tween 20 (TBST) buffer containing 5% BSA, washed with TBST three times, and then incubated overnight at 4°C with polyclonal anti-NPY (1:1000, Novus Biologicals, NBP1-46535), monoclonal Anti-TH (1:500, Abcam, ab129991) and β-actin antibody (1:1000, Boster, BM0627, China), respectively. After the membranes were washed with TBST, the membranes incubated with the secondary biotin-conjugated antibody and then with anti-biotin horseradish peroxidase (HRP)-linked antibody (1:1000). Finally, protein signals were detected using SuperSignal West Pico Chemiluminescent Substrate Trial kit (Thermo Scientific, No.34079) and quantified by densitometry using Quantity One software (Bio-Rad).

Statistical analysis

The statistical analysis was conducted using SPSS 20.0 for Windows software. Data were present as mean ± standard deviation (SD). Differences in group were analyzed by using repeated measure analysis of variance (ANOVA). $P<0.05$ was considered to be statistical significance.

Table 1. Comparison of PSV, EDV, Vm, Pi and Ri in the bilateral vertebral arteries between the CSA group and the control group

Groups	n		PSV (cm/s)	EDV (cm/s)	Vm (cm/s)	Pi	Ri
Control group	8	Right	18.98±1.33	10.49±0.83	26.53±0.55	1.01±0.05	0.59±0.02
		Left	20.96±2.24	11.30±1.98	27.79±0.80	1.09±0.10	0.64±0.03
CSA group	8	Right	10.91±1.97**	10.24±0.81	13.73±1.61**	1.43±0.11**	0.71±0.08*
		Left	20.65±2.13	10.81±1.45	27.90±0.92	1.08±0.10	0.62±0.05

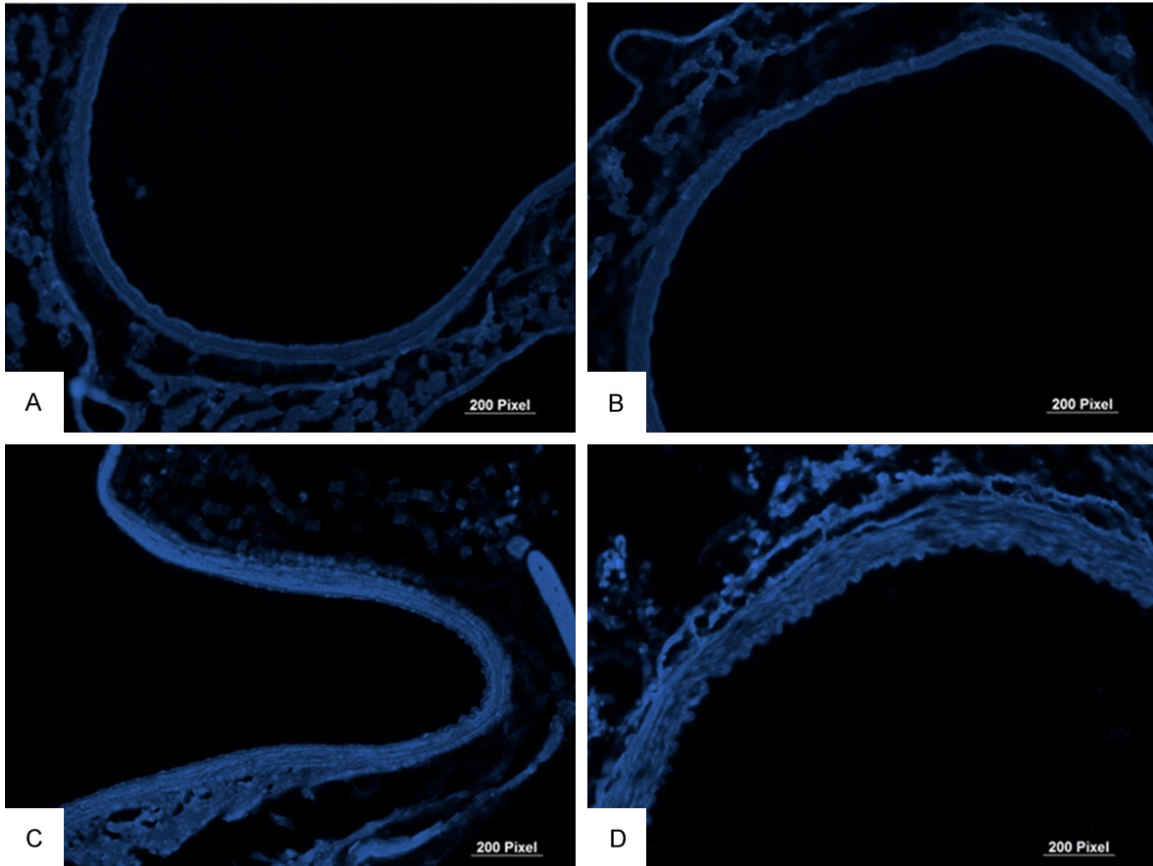*$P<0.05$, **$P<0.01$, as compared with the ipsilateral vertebral artery control group, (Mean ± SD).

Figure 1. Fluorescence micrographs of longitudinal sections of right side vertebral artery in A group (A), B group (B), C group (C) and D group (D).

Results

Transcranial doppler sonography (TCD) recordings

As shown in **Table 1**, the Pi and RI of right vertebral artery in CSA group were remarkably higher than those in control group ($P<0.05$). However, the PSV and Vm of right vertebral artery in CSA group were remarkably lower than those in control group ($P<0.05$). Compared with the left vertebral artery in control group, the PSV, EDV, Pi, Vm and Ri of left vertebral artery in CSA group had no statistically significant difference ($P>0.05$). Those TCD detection results demonstrated that the CSA animal model was successfully induced by injecting sclerosing agent.

Fluorescent tracer fast blue staining

After injected the fluorescent tracer FB for 24 h, there was no or dim fluorescence scattered in the interior walls of the right side vertebral arteries in A group and B group (**Figure 1A**, **1B**), however, some light blue fluorescence was
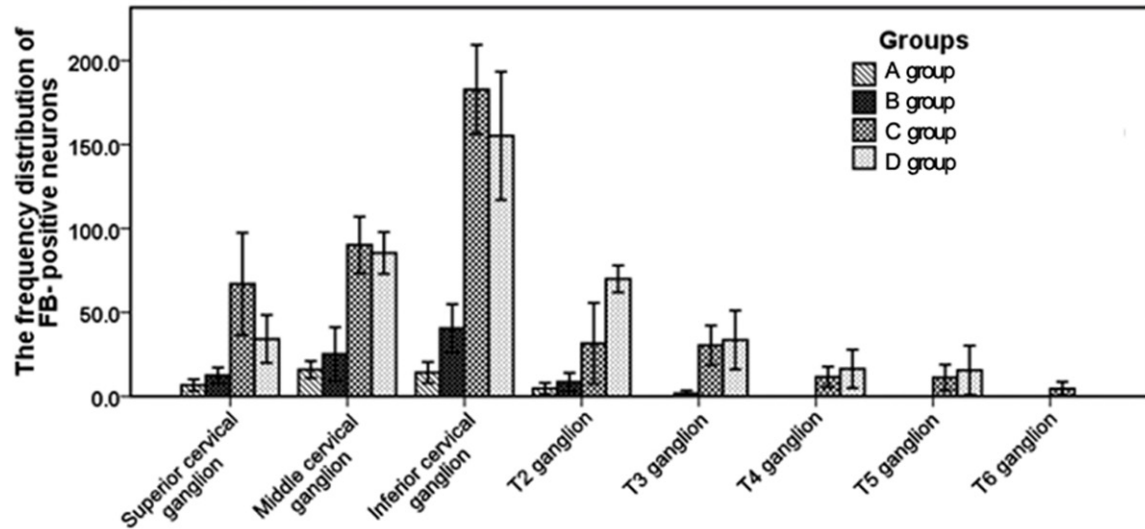
Figure 2. The frequency distribution of FB-positive neurons in each segmental level of the sympathetic trunk ganglia in A group, B group, C and D group.

observed in the interior walls and adventitia of the right side vertebral artery in C group and D group (**Figure 1C**, **1D**). The FB labeled neurons of STG tissue samples were found consistently in the right side superior, middle and inferior cervical ganglion (stellate ganglion). The mean diameter of STG neuronal nuclei of A group, B group, C group and D group was 7.4±1.6 μm, 7.4±1.4 μm, 7.6±1.8 μm and 7.5±1.5 μm, respectively. There was no significant differences among each group (*P*>0.05). The number of FB-positive neurons was calculated by using Abercrombie's formula. The correction factor of A group, B group, C group and D group was 0.73, 0.73, 0.72 and 0.73, respectively. The results shown that merely 36.1±4.1 FB-positive neurons was counted in A group, and 64.8±9.6 FB-positive neurons was counted in B group. By contrast, 312.6±24.4 FB-positive neurons was counted and mostly located in middle and inferior cervical ganglion in C group. Moreover, 299.6±6.9 FB-positive neurons was counted and mostly located in middle and inferior cervical ganglion in D group (**Figure 2**). The number of FB-positive neurons were compared among four groups that exhibited significant difference (*P*<0.01), except the comparison of C group and D group (*P*>0.05).

Fluorescent histochemical staining

After NPY-immunohistorchemical staining, FB-positive neurons were showing green fluorescence. However, FB-positive neurons were labeling red fluorescence by TH-immunohistorchemical staining (**Figure 3**). As shown in **Table 2**, the average percentage of FB-positive neurons co-expressed NPY and TH-immunoreactivity in D group was significantly higher than those in other three groups (*P*<0.05), while the average percentage of FB-positive neurons showing NPY or TH-immunoreactivity has no significantly different among in four groups (*P*>0.05).

NPY and TH protein expression

The protein expressions of NYP and TH were investigated by using western blot analysis. As shown in **Figure 4**, the NYP and TH protein expression in D group were significantly increased compared with the other three groups (all *P*<0.05). However, the NYP and TH protein expression comparison among A group, B group and C exhibited no significant difference (*P*>0.05).

Discussion

CSA is a common type of cervical spondylosis, but its pathogenesis is not completely known. In order to explore the precise mechanism of pathgenisis, build an animal model of CSA is one of very important methods. Many methods to establish the CSA animal model were reported, but the animal studies on simulating CSA were still very limited, due to those methods were defective. Shou et al. [8] reported a practi-
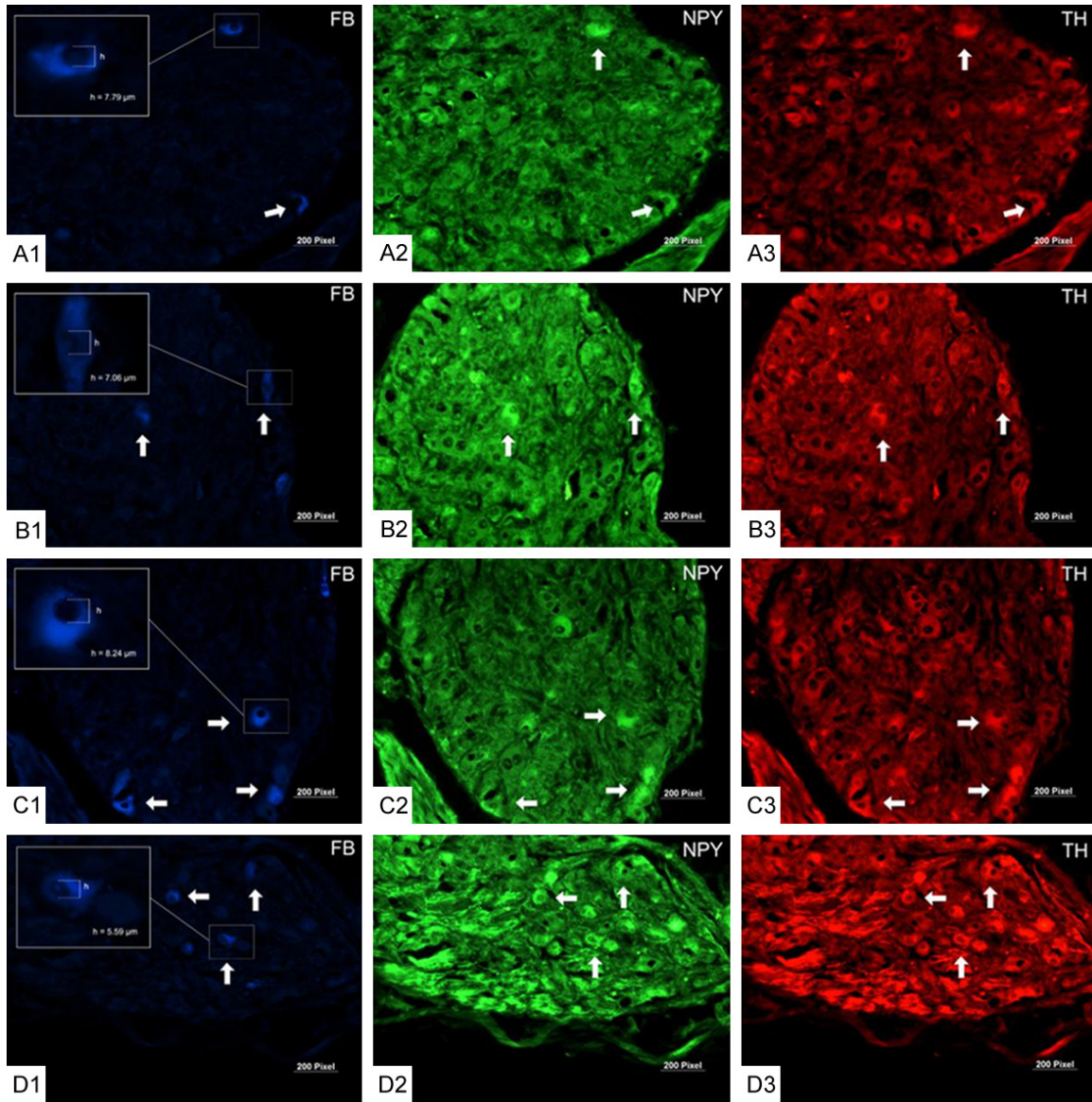
Figure 3. Fluorescence micrographs of longitudinal sections of right side middle cervical ganglion containing FB-positive perikarya double labeled for NYP and TH in A group (A1-3), B group (B1-3), C (C1-3) and D group (D1-3). The arrow points to a FB-positive cell body simultaneously contained NYP and TH.

Table 2. The average percentage of FB-positive neurons showing NPY, TH and co-expressed NPY and TH-immunoreactivity

Percentage (%) Group	NPY-immu-noreactivity	TH-immu-noreactivity	co-expressed NPY and TH-immunoreactivity
A group	61.2±6.0	70.2±9.2	56.1±5.5*
B group	64.2±5.9	70.7±6.6	58.0±7.8*
C group	68.2±5.8	74.1±4.2	60.5±3.9*
D group	77.8±6.7	81.9±6.7	69.2±4.6

*$P<0.05$, as compared with the average percentage of FB-positive neurons co-expressed NPY and TH-immunoreactivity of CSA group.

cal method to establish the CSA animal model by mean of injecting Xiaozhiling injection (sclerosing agent, one of prescription drugs for internal hemorrhoid treatment) next to transverse process of cervical vertebra, and their study demonstrated that Xiaozhiling injection was injected into the neck next to the cervical transverse process induced muscle solidification and aseptic inflammation. The muscles that around the cervical
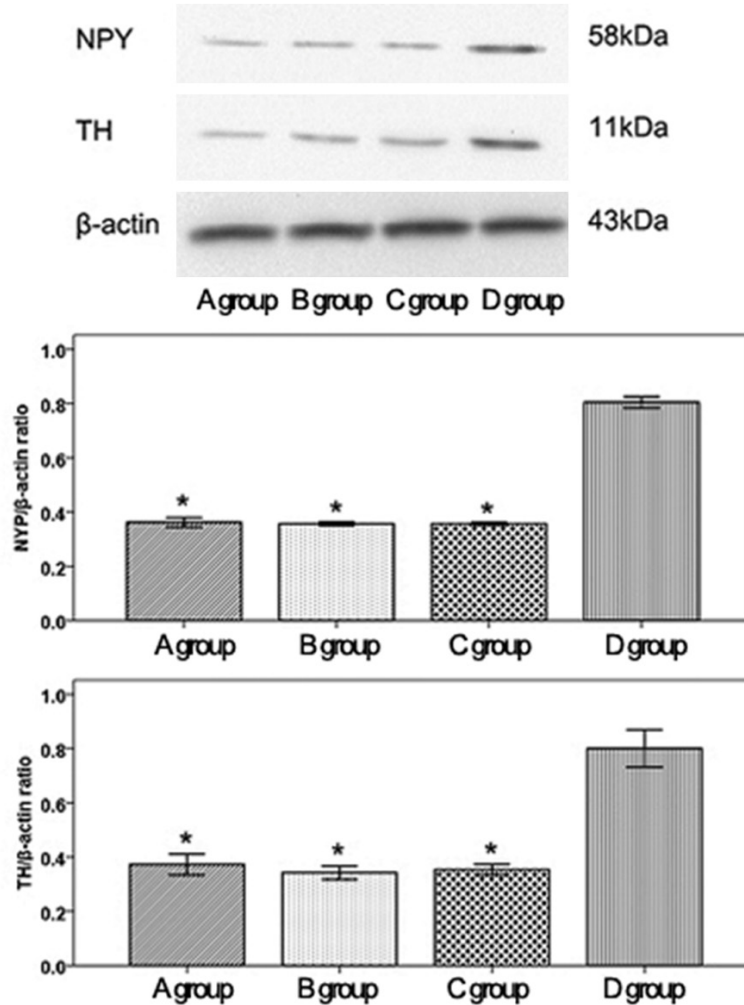
Figure 4. The protein expression of NYP and TH in A group, B group, C group and D group. *P<0.01: significant difference from the CSA group.

normal rabbits (P<0.05). The result of TCD detection suggested that injecting scleroing agent able to induce vertebribasilar insufficiency, and the CSA rabbit models were successfully reconstructed. Moreover, lower dosage of sclerosing agent not only successfully induces the CSA animal model, but it also reduces suffering of experimental animal.

Cervical vertebra degeneration is the pathogenesis basis of the cervical spondylosis. The imbalance of biomechanics in cervical vertebrae is the primary mechanisms of cervical vertebra degeneration, and it as a result of the change of cervical vertebrae physiological curvature and cervical vertebrae instability that induced by bilateral neck muscle abnormalities, facet joints instability, and so on. Cervical sympathetic nerve around the vertebral artery and regulate the blood flow [13], in particular, vertebral nerve is the biggest one. In case of cervical sympathetic nerve was stimulated by the imbalance of biomechanics in cervical vertebrae, and that would induce vasoconstriction, vasospasm and oligemia of the vertebral artery. Moreover, the higher distribution density of reticular nerve fibers, which are made up of sympathetic nerve branches derive from middle and inferior cervical ganglion (stellate ganglion), are surrounding the C3-C5 cervical sections of vertebral artery. Those sections of vertebral artery were very susceptible to external pathologic factors, such as Luschka joint hyperplasia, cervical facet jionts displacement and neck spasms. Neck soft tissues (such as muscles, tendons, ligaments) and facet joints maintain the physiological curvature and stability of cervical vertebrae. Some scholar suggested that vertebral artery stimulated by different kinds of pathogenic factor was susceptibility to cause the vertebral artery

transverse process in injection site were deprived the extension and contraction function, and it led to cervical unstability and facet joints instability. Local aseptic inflammation in neck can promote the disc degeneration [11] and stimuli the cervical sympathetic nerve [12]. The excited sympathetic nerve is an importance factor for insufficiency of blood supply in the vertebral basilar artery. In the present study, Xiaozhiling injection was injected into the right side of neck next to the cervical transverse process as previous study [8]. To investigate the diagnosis of CSA in rabbits, the TCD detection was performed after 4 weeks of last time to inject sclerosing agent. Pi and RI of right vertebral artery were remarkably higher, and PSV and Vm of right vertebral artery in CSA rabbit model were remarkably lower than those in

blood-supply insufficiency than stimulated by mechanical compress. The effect of lesion in neck soft tissues or cervical facet joints on vertebral artery and sympathetic nerve should be further studied. Thus, in the present study, we observed the sympathetic nerve around the vertebral artery, cervical, thoracic and lumbar STG using fluorescent tracer FB. FB was injected in different injection sites to imitate the lesions or inflammation in hypoderm, upper trapezius muscle and next to parapophysis of cervical vertebra that on the C3-C5 cervical sections. light blue fluorescence was found in the interior walls and adventitia of the right side vertebral artery in the rabbits after injected FB next to parapophysis of cervical vertebra. However, no or dim fluorescence was found in the interior walls of the right side vertebral artery after FB was injected in hypoderm or upper trapezius muscle. Subsequently, the number of FB-positive neurons in right side STG was calculated, and demonstrated that a large number of FB-positive neurons were observed in the rabbits after injected FB next to parapophysis of cervical vertebra, and there was no significant difference between C group and D group. The FB-positive neurons were found in right side cervical STG and ipsilteral thoracic STG. However, there was only a few number of FB-positive neurons were observed in the rabbits with FB-hypodermic injection (A group) or FB-intramuscular injection (B group). Upper trapezius muscle is innervated by accessory nerve and cervical nerve (C2-C4). Neck hypoderm is innervated by cutaneous nerve which stem from brachial plexus. It has been confirmed that there was a certain relationship between cervical spinal nerve and cervical sympathetic nerve [14]. We speculated that the light blue fluorescence intensity in vertebral artery and number of FB-positive neurons in STG indicated that different lesion sites in neck tissue make different effect on vertebral artery and STG, due to different sympathetic nerve density and lesion extent. The density of sympathetic nerve around transverse process of cervical vertebra is higher than hypoderm and upper trapezius muscle. As result of the sympathetic nerve around vertebral artery was directly activated, cervical facet jionts lesion as one of pathogenic mechanisms of CSA may cause severe vertebral artery spasm and stenosis. Of course, the cause of CSA is various. If, for instance, the lesion in upper trapezius muscle continues to worsen, that it would finally cause insufficient blood-supply of vertebral-basilar artery.

Neuropeptide Y (NPY) is an important neurotransmitter involves in neurovascular regulation and secreted from sympathetic nerve [15]. NPY also is a vasoconstrictor, and not only exhibits directly effect on contraction of vascular smooth muscle but also reinforces the vasoconstriction of other vasoconstrictor [16]. Tyrosine hydroxylase (TH) is the first reported enzyme in tyrosine synthesis, which exists in the cytoplasm of adrenergic nerve cells. TH serves as the speed limit enzymes and plays a role in catalyst. In many previous studies, NPY and TH were used as specific markers of sympathetic nerve [17]. The sustained excitement of sympathetic nerves induced the NPY release increased and the TH activity up-regulated. To further investigate the sympathetic function in CSA rabbit model, the fluorescent histochemical staining and the protein expression of NPY and TH was conducted. The average percentage of FB-positive neuron double immunolabled for NPY and TH in CSA rabbit model was higher than other normal rabbits. Subsequently, the western blotting result shown that both the protein expression of NPY and TH in CSA rabbit model was significant higher than other normal rabbits ($P<0.01$). From those results, we speculated that right side sympathetic nerve of CSA rabbit model was stimulated by muscle solidification, aseptic inflammation and facet joints instability, and the expressions of NPY and TH remarkable increased. Finally, vasoconstriction, vasospasm and oligemia of the ipsilateral vertebral artery occurred.

In summary, the present study proves once again the method to establish the CSA animal model by mean of injecting sclerosing agent next to parapophysis of cervical vertebra is easy to operate and could effectively simulating the pathogenesis of CSA as human situations in nearly a real. Most importantly, it is the first time using retrograde-tracing and immunohistochemical study to demonstrate that cervical facet lesion may cause severe vertebral artery spasm and stenosis contrast with other lesion sites in neck tissue, due to the sympathetic nerve around vertebral artery was directly activated in CSA rabbit model.

Disclosure of conflict of interest

None.

Address correspondence to: Lehua Yu, Department of Rehabilitation Medicine and Physical Therapy, The Second Affiliated Hospital, Chongqing Medical University, Chongqing, China. Tel: +86 1389617-9179; E-mail: yulehua@cqmu.edu.cn

References

[1] Singh S, Kumar D, Kumar S. Risk factors in cervical spondylosis. J Clin Orthop Trauma 2014; 5: 221-226.

[2] Li Y, Peng B. Pathogenesis, Diagnosis, and Treatment of Cervical Vertigo. Pain Phys 2015; 18: E583-95.

[3] Moon ES, Karadimas SK, Yu WR, Austin JW, Fehlings MG. Riluzole attenuates neuropathic pain and enhances functional recovery in a rodent model of cervical spondylotic myelopathy. Neurobiol Dis 2014; 62: 394-406.

[4] Karadimas SK, Moon ES, Yu WR, Satkunendrarajah K, Kallitsis JK, Gatzounis G, Fehlings MG. A novel experimental model of cervical spondylotic myelopathy (CSM) to facilitate translational research. Neurobiol Dis 2013; 54: 43-58.

[5] Hirai T, Uchida K, Nakajima H, Guerrero AR, Takeura N, Watanabe S, Sugita D, Yoshida A, Johnson WE, Baba H. The prevalence and phenotype of activated microglia/macrophages within the spinal cord of the hyperostotic mouse (twy/twy) changes in response to chronic progressive spinal cord compression: implications for human cervical compressive myelopathy. PLoS One 2013; 8: e64528.

[6] Steffen F, Voss K, Morgan JP. Distraction-fusion for caudal cervical spondylomyelopathy using an intervertebral cage and locking plates in 14 dogs. Vet Surg 2011; 40: 743-752.

[7] Klironomos G, Karadimas S, Mavrakis A, Mirilas P, Savvas I, Papadaki E, Papachristou DJ, Gatzounis G. New experimental rabbit animal model for cervical spondylotic myelopathy. Spinal Cord 2011; 49: 1097-102.

[8] Shou Z, Shen L, Xiong P. Assessing the validity of a novel model of vertebral artery type of cervical syndrome induced by injecting sclerosing agent next to transverse process of cervical vertebra. J Huazhong Univ Sci Technolog Med Sci 2010; 30: 85-88.

[9] Ragionieri L, Botti M, Gazza F, Sorteni C, Chiocchetti R, Clavenzani P, Minelli LB, Panu R. Localization of peripheral autonomic neurons innervating the boar urinary bladder trigone and neurochemical features of the sympathetic component. Eur J Histochem 2013; 57: e16.

[10] Guillery RW. On counting and counting errors. J Comp Neurol 2002; 447: 1-7.

[11] Demircan MN, Asir A, Cetinkal A, Gedik N, Kutlay AM, Colak A, Kurtar S, Simsek H. Is there any relationship between proinflammatory mediator levels in disc material and myelopathy with cervical disc herniation and spondylosis? A non-randomized, prospective clinical study. Eur Spine J 2007; 16: 983-986.

[12] Liu MH, Tian J, Su YP, Wang T, Xiang Q, Wen L. Cervical sympathetic block regulates early systemic inflammatory response in severe trauma patients. Med Sci Monit 2013; 19: 194-201.

[13] de Souza Faleiros AT, de Abreu Maffei FH, de Lima Resende LA. Effects of cervical sympathectomy on vasospasm induced by meningeal haemorrhage in rabbits. Arq Neuropsiquiatr 2006; 64: 572-4.

[14] Zuo J, Han J, Qiu S, Luan F, Zhu X, Gao H, Chen A. Neural reflex pathway between cervical spinal and sympathetic ganglia in rabbits: implication for pathogenesis of cervical vertigo. Spine J 2014; 14: 1005-1009.

[15] Hodges GJ, Jackson DN, Mattar L, Johnson JM, Shoemaker JK. Neuropeptide Y and neurovascular control in skeletal muscle and skin. Am J Physiol Regul Integr Comp Physiol 2009; 297: R546-555.

[16] Gradin KA, Buus CL, Li JY, Frøbert O, Simonsen U. Neuropeptide Y2 receptors are involved in enhanced neurogenic vasoconstriction in spontaneously hypertensive rats. Br J Pharmacol 2006; 148: 703-713.

[17] Decressac M, Pain S, Chabeauti PY, Frangeul L, Thiriet N, Herzog H, Vergote J, Chalon S, Jaber M, Gaillard A. Neuroprotection by neuropeptide Y in cell and animal models of Parkinson's disease. Neurobiol Aging 2012; 33: 2125-2137.